Preliminary Analysis for Determination on the Flow Path of SMART Core Shielding Structure

Y.M. JEON [a*], Y.G. KIM [a], Y.M. BAE [a], Y.I. KIM [a], C.T. PARK [a], S. CHOI [a]
[a]*Korea Atomic Energy Research Institute, 150-1 Dukjin-dong, Yuseong-Gu, Daejeon 305-353, Republic of Korea*
[*]*Corresponding author: jeonym85@kaeri.re.kr*

1. Introduction

SMART is an integral type nuclear cogeneration reactor having been developed in Korea [1]. A core support barrel assembly of reactor internal structure is composed of a core support barrel, a lower core support plate and a core shroud assembly in SMART. To enhance the neutron utilization and to reduce the neutron influence to the reactor vessel and steam generators [2], a shielding structure is installed in the space between the core shroud and the core support barrel. Various types of cooling flow paths could be applied to ensure the effective cooling for the shielding structure. In this paper, the cooling performances are evaluated for several basic types of shielding structures. Based on the present result, an optimized flow path design for shielding structure is proposed.

2. Approaches

2.1 Numerical analysis method

In this numerical simulation, it is assumed that the flow is steady state and 3D-1/8 axisymmetric in reactor and the fluid is incompressible. In addition, gravity is considered and material properties variation with temperature such as viscosity and density are reflected. The commercial CFD code, Fluent 12.0, is applied to solve incompressible governing equations. The governing equations are described as follows:

Conservation of mass (continuity equation)

$$\frac{\partial}{\partial x_i}(\rho u_i) = 0 \tag{1}$$

Conservation of momentum

$$\frac{\partial}{\partial x_j}\left(\rho u_i u_j\right) =$$

$$-\frac{\partial \boldsymbol{p}}{\partial x_i} + \frac{\partial}{\partial x_j}\left[\mu\left(\frac{\partial u_i}{\partial x_j} + \frac{\partial u_j}{\partial x_i} - \frac{2}{3}\delta_{ij}\frac{\partial u_l}{\partial x_l}\right)\right]$$

$$+\frac{\partial}{\partial x_j}\left(-\rho\overline{u_i' u_j'}\right) + \boldsymbol{G}_b \tag{2}$$

Conservation of energy

$$\frac{\partial}{\partial x_i}[u_i(\rho \boldsymbol{E} + \boldsymbol{p})] =$$

$$\frac{\partial}{\partial x_j}\left[\left(k + \frac{\boldsymbol{C_p}\mu_t}{\boldsymbol{Pr}_t}\right)\frac{\partial \boldsymbol{T}}{\partial x_j} + u_i\left(\boldsymbol{\tau}_{ij}\right)_{eff}\right] + \boldsymbol{S}_h \tag{3}$$

Realizable k-ε turbulence models [3] are investigated in this study. And the CFD analysis is performed using following methods.

- Wall mesh option: standard wall function
- Discretization: Second order upwind (Momentum, Turbulence, Energy), Standard (Pressure)
- Pressure-velocity coupling: SIMPLE algorithm
- Solver: Single precision solver

2.2 Configuration

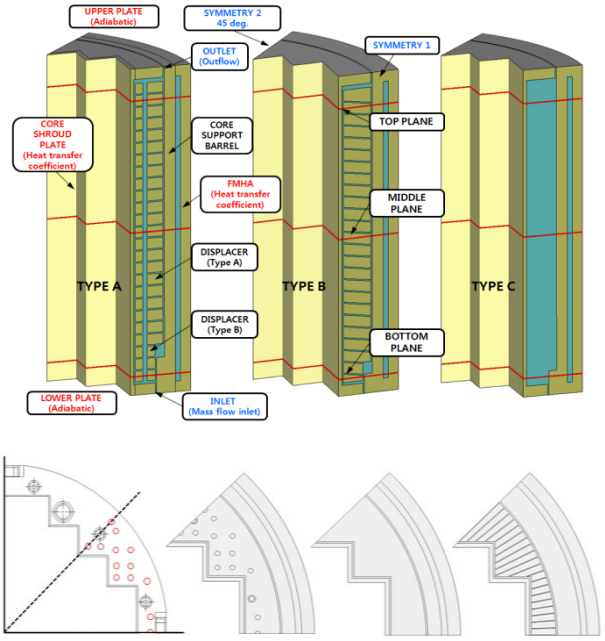

Fig. 1 Configurations and boundary conditions

As representative cases, simplified three shapes of the shielding structure are considered. The geometries and the boundary conditions for the three cases are shown in fig. 1. Plates having several flow holes to enhance cooling effect are horizontally installed in Type-A. Horizontal plates with a gradient of 10 degrees to improve the natural convection performance are considered in Type-B. Vertical plates are applied in Type-C to improve the cooling capability by supplying finely dispersed vertical flow. Boundary conditions of heat transfer coefficient on the inner-outer wall, adiabatic on the top-bottom wall, and symmetry on the side wall in the calculation domain are considered to simplify the problem.

2.3 Grid Composition

The hexagonal prism mesh is generated by using

Gambit 2.4 as shown in fig. 2 and fig. 3. Volume cells from 18 to 41 million are used for these simulations. As shown in fig. 2, pave meshes are used on the horizontal section in the shielding structure part, map meshes are employed on other horizontal section of the shielding structure parts. The rectangular map meshes utilized on the axial plane are displayed in fig. 3. Grid dependency is checked using two difference mesh resolutions of 26 million and 41 million for Type-C. The more detail investigation for the influences of grid and turbulence models et al. will be performed in the next analysis for the selected shielding structure.

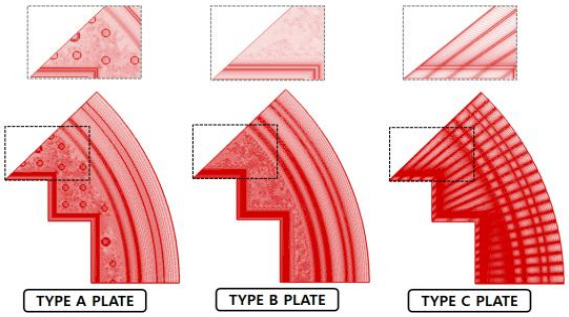

Fig. 2 Grid distribution on horizontal planes

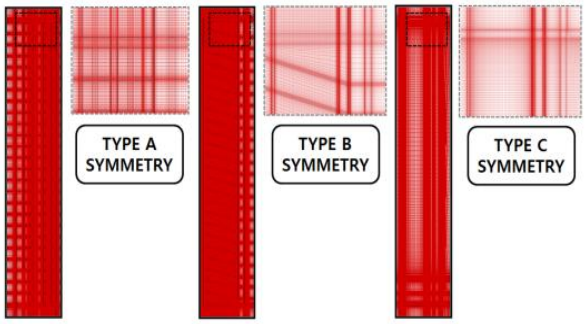

Fig. 3 Grid distribution on vertical planes

3. Result and Discussion

To choose the shielding structure that is excellent in cooling effect, the temperature distributions in shielding structures and flow paths are compared. Figure 4 shows the comparison of the temperature distribution on the top, bottom and symmetry plane of fig. 1. The lowest temperature distribution on the top, middle and bottom plane is shown in the Type-C shielding structure and the highest temperature distribution on those planes is revealed in the Type-B. The Type-A structure shows similar distribution to the Type-C. Considering of the temperature on the top, middle and bottom plane, Type-A and Type-C plane showing satisfactory results for the cooling performance could be candidates as the type of shielding structure. The detail design optimization such as reducing stagnation flow patterns appearing in the bottom region or flow balancing inner and outer space is scheduled for future work. Table 1 shows the maximum values of temperature at the planes in shielding structures.

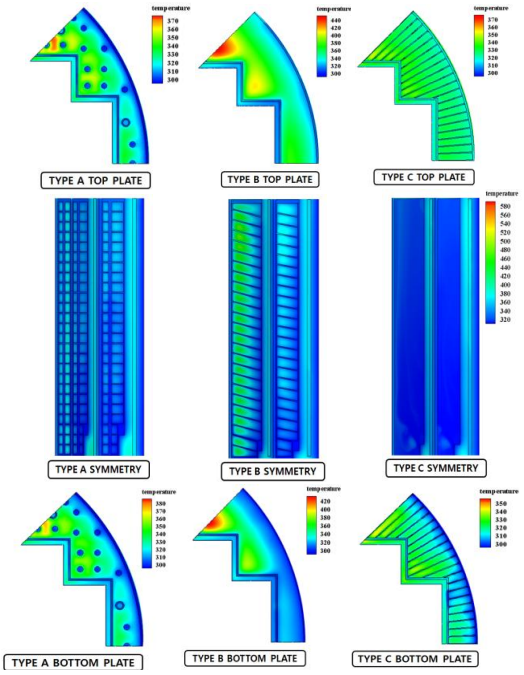

Fig. 4 Temperature distribution on top, bottom and symmetry planes

Table 1 Comparison of maximum temperatures

CASE	Maximum Temperature (℃)		
	TYPE A	TYPE B	TYPE C
Top	390.7	444.4	372.4
Middle	383.5	417.9	359.2
Bottom	390.7	428.1	358.1

4. Conclusions

CFD analysis is performed using Fluent 12.0 to determine the flow path of the shielding structure showing higher cooling capability in SMART. As a result, horizontal plates with several flow holes and vertical plates are selected as the candidates of core shielding structure of SMART. Based on the present result, the detail design optimization for the flow path in the core shielding structure will be performed in further work.

Acknowledgement

This study has been performed under a contract with the Korean Ministry of Educational Science and Technology.

REFERENCES

[1] G.G. KIM, S.G. JI, Small and Medium Integral Reactor, SMART Development, Journal of the Computational Structural Engineering Institute of Korea, Vol. 21, p.23-29, 2008
[2] M.H. Chang, SMART Behavior under Over-Pressurizing Accident Conditions, Nuclear Engineering and Design 199, p.187-196, 2000
[3] ANSYS, Inc., Fluent 12.0 Manual, 2010.